Angular-modulated spatial distribution of ultrahigh-order modes assisted by random scattering*

Xue-Fen Kan(阚雪芬)[1], Cheng Yin(殷澄)[1,2,†], Tian Xu(许田)[3], Fan Chen(陈凡)[4], Jian Li(李建)[1], Qing-Bang Han(韩庆邦)[1], and Xian-Feng Chen(陈险峰)[2]

[1] *Jiangsu Key Laboratory of Power Transmission and Distribution Equipment Technology, Hohai University, Changzhou* 213022, *China*
[2] *The State Key Laboratory on Fiber Optic Local Area Communication Networks and Advanced Optical Communication Systems, Department of Physics and Astronomy, Shanghai JiaoTong University, Shanghai* 200240, *China*
[3] *Physics Department, Nantong University, Nantong* 226007, *China*
[4] *Optoelectronics Devices Laboratory, Photonlabs Inc., Shanghai* 201843, *China*

(Received 27 May 2017; revised manuscript received 21 June 2017; published online 30 September 2017)

In designing an optical waveguide with metallic films on a nanometer scale, the random scattering by the natural roughness of the thin film is always ignored. In this paper, we demonstrate that for the ultrahigh-order modes (UOMs) in the symmetric metal cladding waveguide, such a scattering leads to drastic variations in their spatial distribution at different incident angles. Owing to the high mode density of the UOMs, the random scattering induced coupling can be easily related to different modes with different propagation directions or wavenumbers. At small incident angles, the intra-mode coupling dominates, which results in a spatial distribution in the form of concentric rings. At large incident angles, the inter-mode coupling plays the most important role and leads to an array-like pattern. Experimental evidence via optically trapped nanoparticles support the theoretical hypothesis.

Keywords: metallic waveguide, random scattering, optical trapping

PACS: 42.79.Gn, 87.80.Cc, 52.25.Tx **DOI:** 10.1088/1674-1056/26/11/114210

1. Introduction

Ultrahigh-order modes (UOMs) are the unique oscillating modes confined between two metallic films in a slab optical waveguide on a millimeter scale in thickness, which is also known as the symmetric metal-cladding waveguide (SMCW).[1] These modes can be excited via free space coupling,[2] and their high intensities due to the enhancement of the waveguide have been applied successfully to precision metrology,[3,4] biomedical detection,[5] Raman scattering,[6,7] etc. Besides, the UOMs are also interesting in many other aspects, such as Goos–Hanchen shift,[8] magneto-optical effect,[9] slow light,[10] and so on. To the best of our knowledge, the spatial distribution of the UOMs has not been investigated, which may be crucial in various potential applications relating to the mode-matter interaction, e.g., the optical manipulation of massive nanoparticles.[11] In this paper, experiments are carried out to investigate the spatial distribution of the UOMs via optically trapped nanoparticles, whose density is proportional to the local field intensity. In principle, a well collimated laser beam can only excite one specific UOM, whose propagation constant matches well with the transversal component of the incident wavevector. However, the pattern of the trapped nanoparticles reveals that multi-modes are excited, which, we believe, is due to the random scattering from the natural roughness of the nanometer thick metallic coupling layer. Furthermore, experiments demonstrated two different patterns under different incident angles, which indicates that the spatial distribution of the UOMs is angular dependent.

The ability to control and adjust the optical field landscape is important when achieving ultra-gentle manipulation of the small trapped objects, which has aroused a widespread current interest. For example, holographic optical tweezers (HOTs),[12,13] which rely on the use of holographic elements to create a specific function of the optical field, provide an effective method to generate a variety of optical traps for dynamic manipulation[14,15] of the colloidal particles, biological cells, virus, etc. Other technologies adopt Ince–Gaussian beams[16] or doughnut beams[17] to increase the versatility in a range of possible optical landscapes. Consequently, our finding may prove the possibility of optical manipulation of colloidal particles via slab waveguides, which possesses many advantages such as field enhancement, versatile structural design, easy modulation, and has not been applied to this field yet. The rest of this paper is arranged as follows. In Section 2, the physics behind the two coupling mechanisms is discussed in detail after a brief summary of the UOMs. Then in Section 3 we describe the experimental process and discuss the observed phenomenon. Finally, some conclusions are drawn from the present studies in Section 4.

*Project supported by the National Natural Science Foundation of China (Grant Nos. 11404092 and 11574072) and the Natural Science Foundation of Jiangsu Province, China (Grant Nos. BK20140246 and BK20160417).

†Corresponding author. E-mail: cyin.phys@gmail.com

© 2017 Chinese Physical Society and IOP Publishing Ltd

2. Theoretical analysis

The basic structure of the SMCW chip is composed of a guiding layer and two metal films, which are used as cladding layers. The SMCW used in this paper is shown in Fig. 1, where the 30-nm-thick upper silver film is deposited on a 0.3-mm-thick thin glass slab and used as coupling layer. Another 200-nm-thick silver film works as a substrate, and a 0.7-mm-thick sample room with inlet and outlet design is also filled with nanoparticle colloid.

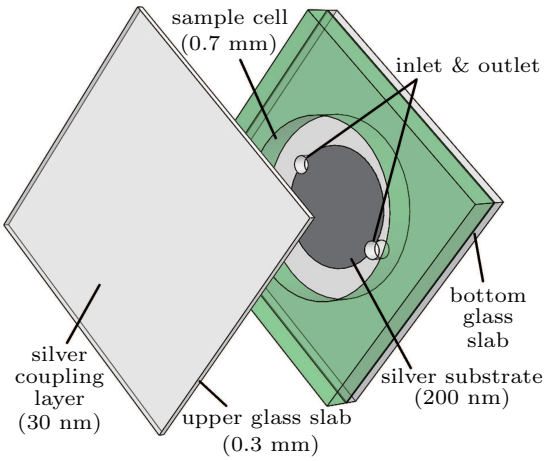


Fig. 1. (color online) Schematic diagram of the hollow-core metal cladding waveguide.

The mode eigenequation of the SMCW can be approximated by a simplified three-layer model, i.e., the leakage from the coupling layer is ignored. For the TE mode, the eigenequation can be written as[18]

$$\kappa_1 d = m\pi + 2\arctan\left(\frac{\alpha_2}{\kappa_1}\right), \tag{1}$$

while for TM mode, the eigenequation takes the form of

$$\kappa_1 d = m\pi + 2\arctan\left(\frac{\varepsilon_1\alpha_2}{\varepsilon_2\kappa_1}\right), \tag{2}$$

where κ_1 is defined by $\kappa_1 = \sqrt{k_0^2\varepsilon_1 - \beta^2}$, α_2 is the decay factor in metallic film and can be written as $\alpha_2 = \sqrt{\beta^2 - k_0^2\varepsilon_2}$, d is the thickness of the guiding layer, m denotes the mode index, ε_1 and ε_2 are the dielectric constants of dielectric and metal, respectively. The propagation constant $\beta = k_0\sqrt{\varepsilon_0}\sin\theta_i$ is related to the effective index n_{eff} of the UOM, and can approach to zero,

$$0 < n_{\text{eff}} = \frac{\beta}{k_0} < \sqrt{\varepsilon_1}, \tag{3}$$

which indicates that there is also no lower limit for the excitation angle θ_1 of the UOM. Free space coupling technology can be used to excite the UOMs, where a laser beam is transmitted directly from free space to the coupling film of the waveguide. It should also be noted that the UOMs are polarization independent, for the guiding layer thickness is on a millimeter scale, i.e., both the second terms on the right-hand side of Eqs. (1) and (2) can be ignored for large value of m ($\sim 10^3$). Theoretically, a well collimated laser beam can only excite one mode, i.e., the eigenequation can only present one propagation constant β when the k_0 and θ_1 are fixed. However, the practical case is significantly different due to the mode coupling mechanism and the random scattering by the roughness of the thin coupling film.

In order to discuss the coupling between different UOMs, we consider the UOM excitation and coupling in $\boldsymbol{k}$-space. As shown in Fig. 2(a), the direction of the incident plane wave is specified by spherical angle (θ, φ), and β is the in-plane component of the incident wave vector $\boldsymbol{k}_0$. Let β_m and β_{m+1} denote the wavenumbers of the $(m+1)$-th and m-th UOMs, respectively, which form two concentric rings by varying the azimuth angle φ as shown in Fig. 2(b). Here in this paper, a specific UOM of $(m+1)$-th order is imagined to be excited via the incident laser beam, whose wavenumber is plotted as β_{m+1}. In Fig. 2(b), it is clear that two different kinds of couplings exist due to the effect of random scattering, i.e., one scatters the wavenumber β_{m+1} to β_m by $\Delta\kappa_1$, and the other scatters the wavenumber β_{m+1} to β'_{m+1} by $\Delta\kappa_2$. In the first case, the mode order is changed, while the propagation direction remains unchanged, and we refer to this case as inter-mode coupling. In the second case, the mode order is not varied but the propagation constant is different, and this effect is called intra-mode coupling. Both scattering wavenumbers $\Delta\kappa_1$ and $\Delta\kappa_2$ can be attributed to the scattering by roughness on the coupling film.

The scattering $\Delta\kappa_{\text{inter}}$ is related to the adjacent UOMs of different orders, which can be solved approximately by the eigenequation, which can be written as

$$\sqrt{k_0^2\varepsilon_1 - \beta_m^2}\,d = m\pi, \tag{4}$$

This equation has ignored the polarization and it follows

$$\begin{aligned}\Delta\kappa_{\text{inter}} &= \frac{\mathrm{d}\beta_m}{\mathrm{d}m} = -\frac{\sqrt{k_0^2\varepsilon_1 - \beta_m^2}}{\beta_m}\pi \\ &= -\frac{\pi}{d}\sqrt{\frac{\varepsilon_1}{\varepsilon_0\sin^2\theta_m} - 1},\end{aligned} \tag{5}$$

where θ_m is the excitation angle of m-th UOM and ε_0 denotes the dielectric constant of the free space. So from Eq. (5), the $\Delta\kappa_{\text{inter}}$ decreases as the incident angle increases. The minus sign in Eq. (5) is due to the fact that $|\beta_{m+1}| < |\beta_m|$, which is also shown in Fig. 2(b). A similar conclusion can be drawn from the reflection spectrum calculated by the transfer matrix method, where the mode density, i.e., number of UOMs per degree of incident angle is much lower at small incident angle. It is obvious from Fig. 3 that the mode density in the range [18°, 20°] is much higher than the range of [0°, 3°], which indicates that the wavenumber difference between adjacent UOMs decreases monotonically. It can be strictly proved

that the interval between two adjacent excitation angles of the UOMs decreases monotonically as long as the incident angle is smaller than 45°, while in our experiments the excitation angle of the UOM will not exceed this limit.

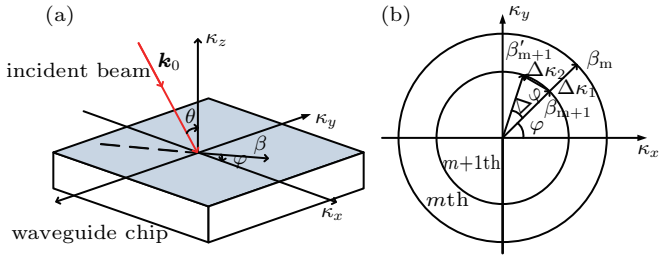


Fig. 2. (color online) Mechanism of the intra-mode and inter-mode coupling. (a) The wave vector $\boldsymbol{k}_0$ of the incident beam and the in-plane propagation constant β in the three-dimensional coordinate system. (b) The intra-mode and inter-mode coupling on the XY plane.

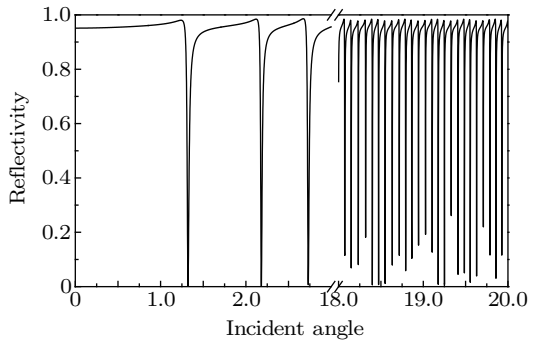


Fig. 3. Numerical simulated reflectivities in ranges of [0°, 3°] and [18°, 20°], respectively. The parameters in the simulation are given as follows: the silver film thickness is $d_{ag} = 30$ nm, the thickness values of the two layers in the guiding layers are $d_{glass} = 30$ mm and $d_{air} = 0.7$ mm, respectively, the incident wavelength is 785 nm, and the dielectric constants are $\varepsilon_{ag} = -23.82 + 1.78\mathrm{i}$, $\varepsilon_{glass} = 2.283$, respectively.

The $\Delta\kappa_{intra}$ corresponds to the coupling between UOMs in different propagation directions, and from Fig. 2(b) it can be approximated by

$$\Delta\kappa_{intra} = \beta_m \Delta\varphi = k_0\sqrt{\varepsilon_0}\Delta\varphi \sin\theta_m. \tag{6}$$

Clearly, the intra-mode coupling requires a scattering magnitude proportional to the sine of the incident angle. So Eqs. (5) and (6) prove that the scattering magnitudes for the two coupling mechanisms depend differently on incident angle. Now we assume that the average magnitudes of the random scattering by the metal film roughness are the same in all the directions, and the incident angle of the laser beam is invariant. Then at small incident angle, $\Delta\kappa_{intra}$ is smaller than $\Delta\kappa_{inter}$, indicating that the intra-mode coupling is easier than the inter-mode coupling. A contrary conclusion can be obtained that the inter-mode coupling is easier at larger incident angle. Furthermore, the spatial distribution of the excited UOMs is not difficult to determine, which is experimentally illustrated by the trapped nanoparticles in the next section. Obviously, at small incident angle, the spatial distribution of the UOMs is of a concentric ring structure when the intra-mode coupling dominates. At large incident angle, inter-mode coupling manifests itself by an array-like distribution of the UOMs.

3. Experiments and discussion

Figure 4 shows the experimental setup. The incident laser beam ($P_{max} = 100$ mW, $\lambda = 785$ nm, TE polarized) is focused directly onto the thin silver film of the SMCW chip after it has passed through two apertures. Then the reflected laser beam is recorded by a photoelectric detector. The SMCW chip is placed on a computer controlled $\theta/2\theta$ goniometer to carry out angular scanning for best coupling. Based on the polarization independent characteristics of the SMCW chip, the polarization of the reflected beam is not considered. Gold nanoparticle solution is injected into the sample room, whilst the particles are optically trapped due to the field enhancement effect of the waveguide structure. The central size of the nanoparticles is 40 nm following the normal distribution and the density of the solution is 0.0019 μg/ml.

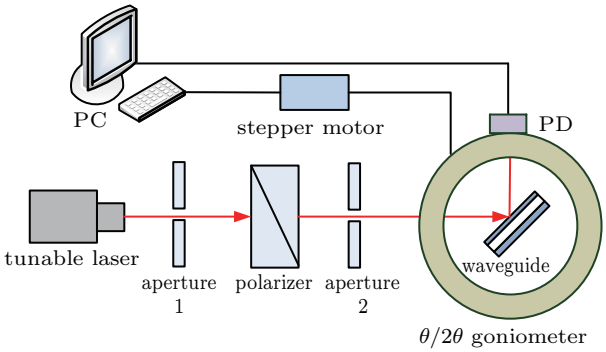


Fig. 4. (color online) Schematic diagram of the experimental setup.

In experiment, the reflectivity is detected so that a specific UOM can be well excited by fixing the incident angle to a reflection dip. Then the experimental setup is kept unchanged until the liquid in the sample room is evaporated completely. The room temperature is fixed at 20° by an air condition. Finally, we remove the upper glass slab carefully and observe the micro-structure formed by the trapped nanoparticles, which has the same pattern as the optical distribution.

Figure 5 illustrates a concentric ring structure of the nanoparticles, whilst the incident angle is around 4°. This result fits well with our hypothesis and proves that the intra-mode coupling dominates at a small incident angle. A concentric ring structure of the nanoparticles is formed in Fig. 5, which is in good accordance with the theoretical prediction of the intensity distribution of UOMs discussed above. It is also noted here that the whole structure is small, for the propagation constant is very small at a near-normal incidence. We have used this feature of UOMs to realize the slow light effect.[10] Hence, a circle is formed by the same order of UOM

propagating in all the directions, while different circles are related to UOMs of different orders.

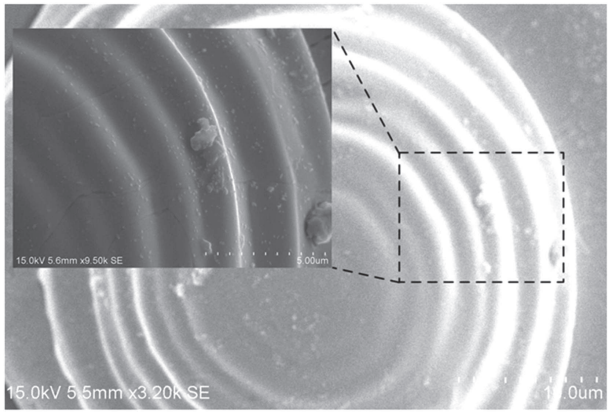


Fig. 5. SEM images of the assembly of nanoparticles under the UOMs excited at small incident angle (insert shows the amplified image of a local structure).

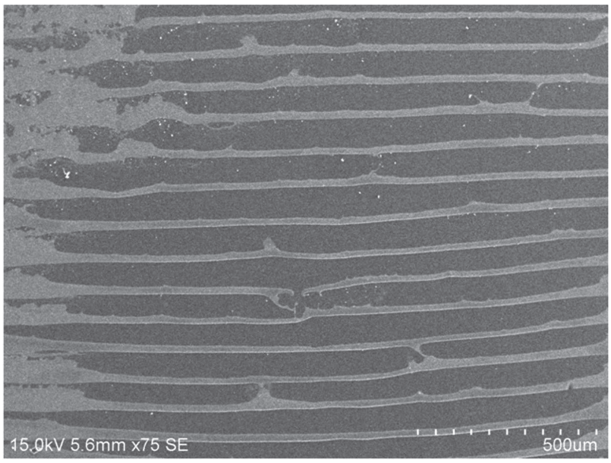


Fig. 6. SEM image of the guided mode assembled morphologies of the trapped particles at large incident angle.

For the second illustration in Fig. 6, the UOMs are excited with an incident angle around 18°, and the SEM records a pattern of the trapped nanoparticles in an array-like form. This phenomenon agrees well with the above theoretical assumption, and can be explained by the fact that the inter-mode coupling is easier at large incident angle. The particle density on the left-hand side of Fig. 6 is higher, and this can be explained by the fact that the SMCW chip is vertically placed, so the particle density is higher near the bottom. Based on Eq. (6), the scattering magnitude for intra-mode coupling is bigger at large incident angle, so the propagation direction is nearly the same as that for the UOMs of the same order, i.e., the magnitude of $\Delta\varphi$ is small. This can be used to explain the almost-straight lines in Fig. 6, while different lines correspond to different orders of the UOMs.

4. Conclusions

By using the SMCW structure, we experimentally demonstrate that the optical distribution pattern can be drastically varied in assisting the random scattering by the natural roughness of nanometer metal film. For this specific waveguide structure, the physics behind the inter- and intra-mode coupling and their relationship with incident angle is thoroughly discussed. Through observing the patterns formed by the optical trapped nanoparticles, we find that the intra-mode coupling at small incident angle leads to a concentric ring structured pattern, while the inter-mode coupling at large incident angle produces an array-like structure. This work is interesting since such a random scattering is usually considered to be undesirable in waveguide design and the applications in optoelectronic devices, communication or sensing. This work may enable potential applications of the traditional slab waveguide in fields such as optical manipulation and optofluidics.

References

[1] Lu H, Cao Z, Li H and Shen Q 2004 *Appl. Phys. Lett.* **85** 4579
[2] Li H, Cao Z, Lu H and Shen Q 2003 *Appl. Phys. Lett.* **83** 2757
[3] Chen L, Cao Z, Shen Q, Deng X, Ou F and Feng Y 2007 *J. Lightwave Technol.* **25** 539
[4] Chen G, Cao Z, Gu J and Shen Q 2006 *Appl. Phys. Lett.* **89** 081120
[5] Sun J, Wang X, Yin C, Xiao P, Li H and Cao Z 2012 *J. Appl. Phys.* **112** 083104
[6] Xu T, Huang L, Yin C, Jin Y, Fang J and Huang M 2014 *Appl. Phys. Lett.* **105** 163703
[7] Yin C, Lu Y, Xu T, Wei D Z, Jin Y L, Fang J H and Huang M Z 2016 *J. Raman Spectrosc.* **47** 560
[8] Wang X, Yin C, Sun J, Li H, Sang M, Yuan W and Huang M 2013 *Appl. Phys. Lett.* **103** 151113
[9] Sun J, Yin C, Zhu C, Wang X, Yuan W, Xiao P and Cao Z 2012 *J. Opt. Soc. Am. B* **29** 769
[10] Yuan W, Yin C, Li H, Xiao P and Cao Z 2011 *J. Opt. Soc. Am. B* **28** 968
[11] Grier D G 2003 *Nature* **424** 810
[12] Grier D G and Roichman Y 2006 *Appl. Opt.* **45** 880
[13] Dufresne E R, Spalding G C, Dearing M T, Sheets S A and Grier D G 2001 *Rev. Sci. Instrum.* **72** 1810
[14] Curtis J E, Koss B A and Grier D G 2002 *Opt. Commun.* **207** 169
[15] Pleguezuelos E, Carnicer A, Andilla J, Martín-Badosa E and Montes-Usategui M 2007 *Comput. Phys. Commun.* **176** 701
[16] Woerdemann M, Alpmann C and Denz C 2011 *Appl. Phys. Lett.* **98** 111101
[17] Ito S, Yamauchi H, Tamura M, Hidaka S, Hattori H, Hamada T, Nishida K, Tokonami S, Ltoh T, Miyasaka H and Lida T 2013 *Sci. Rep.* **3** 3047
[18] Wang X, Yin C and Cao Z 2016 *Progress in Planar Optical Waveguides* (Berlin Heidelberg: Springer) pp. 83–88